Journal of Engineering Physics and Thermophysics, Vol. 74, No. 6, 2001

HEAT EXCHANGE ON THE FRONT SURFACE OF A BLUNT BODY IN A HIGH-SPEED FLOW CONTAINING LOW-INERTIA PARTICLES

É. B. Vasilevskii,[a] A. N. Osiptsov,[b] A. V. Chirikhin,[a] and L. V. Yakovleva[a]

UDC 556.6.071.6:532.529

The method and results of an experimental investigation of the heat exchange on the front surface of a sphere in a supersonic flow containing particles of diameter d = 0.12–2.4 μm and hollow particles of d = 160 μm are presented. It has been revealed that in the case where even very small particles of d = 0.15 μm are contained in an undisturbed flow and their concentration is low (of the order of a percent), the heat flux in the region of the critical point of the model markedly increases. A comparison of the experimental data with the data of calculations of the heat exchange in the region of the forward critical point which are based on the theory of a two-phase laminar boundary layer has been made. A glow near the surface of the model was observed in the experiments conducted in total darkness.

Introduction. A high-speed spacecraft moving in the atmosphere of the earth or other planets can meet with dust or rain-bearing clouds, which can cause additional heating of its surface. The presence of an even small amount of disperse particles in the atmosphere can fundamentally change the structure of the flow near the front surface of a blunt body.

Analogous problems arise in the case of a heterogeneous flow around bodies in different power plants, in plants for producing powder materials, in treatment of surfaces by a two-phase medium, in monitoring of the environment, and in other cases.

In the case of large (inertial) particles and high velocities of the flow considerable erosion of the surface in flow occurs [1]. In experimental investigations of such flows it was noted that the heat flux increases sharply in the region of the forward critical point [2–5]. The indicated investigations were conducted with particles whose size was larger than 30 μm, and only in a small number of experiments was the minimum size of the particles 20 μm [2]. Under these conditions, the intensification of heat exchange is due to three main mechanisms: conversion of the kinetic energy of particles incident on the surface to the heat energy of the body, turbulization of the boundary layer by vortex trails of inertial particles, and additional turbulization caused by the roughness of the surface in flow developing upon impacts of the incident particles.

A theoretical analysis of the motion of particles in the shock layer in the case of flow around a blunt body has shown that low-inertia particles do not find their way to the surface of the body (for example, particles with a diameter of several microns for a diameter of bluntness of the body of 1 m). Such a regime of flow is usually called the regime without inertial precipitation of particles. At the same time, small particles are accumulated in the boundary layer [6]. As a result, with even very low concentrations of particles in an undisturbed flow, the structure of the boundary layer can change markedly and the heat flux in the region of the forward critical point of the body can increase. In the published works known to the authors, there are

[a]N. E. Zhukovskii Central Aerohydrodynamics Institute, Zhukovskii, Moscow Region, Russia; email: vas@tsagi.rssi.ru; [b]Scientific-Research Institute of Mechanics at the M. V. Lomonosov Moscow State University, Moscow, Russia; email: osiptsov@inmech.msu.su. Translated from Inzhenerno-Fizicheskii Zhurnal, Vol. 74, No. 6, pp. 34–42, November–December, 2001. Original article submitted January 9, 2001.

1062-0125/01/7406-1399$25.00

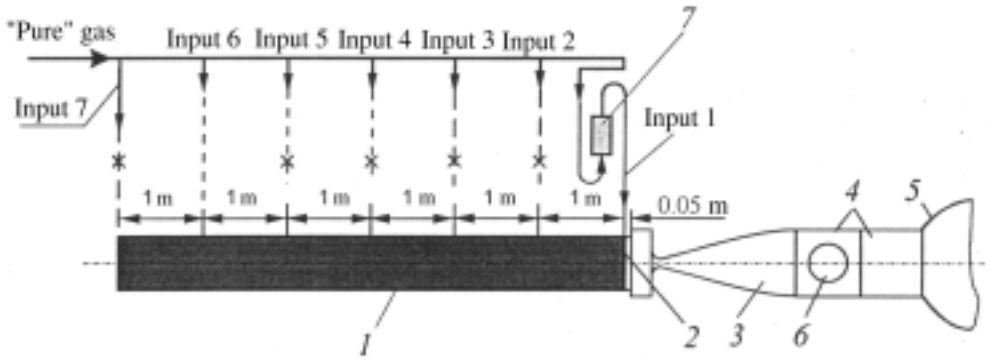

Fig. 1. CAHI UT-1 shock tunnel: 1) high-pressure chamber; 2) diaphragm; 3) nozzle; 4) working portion; 5) vacuum chamber; 6) optical window; 7) mixing device.

no experimental data on the influence of particles on the heat exchange in this range of parameters. The aim of the present investigation is to close this gap.

The experiments were conducted in a UT-1M shock wind tunnel of the Central Aerohydrodynamics Institute (CAHI) according to the Ludwieg scheme. The majority of results have been obtained for a mixture of air with SiO_2 particles with a mean diameter of the particles of d = 0.15 μm. We also used hollow spheres of SiO_2 with an outside radius d = 160 μm and a width of the wall of ~5 μm as well as particles of other substances: Si_3N_4, Fe_2O_3, Cr_2O_3, and Fe with a size d = 0.12–2.4 μm. The weight concentration of the particles in an undisturbed flow varied in the range C = 0–25%. The Reynolds number was $Re_{\infty,R} = (4–500)\cdot 10^3$. As the carrier gas, we used air in the majority of experiments and N_2 and CO_2 in several experiments.

1. Description of the Experimental Setup and the Method. *1.1. UT-1 wind tunnel.* The diagram of the UT-1 shock wind tunnel of the CAHI is shown in Fig. 1. Chamber 1 is equipped with an external ohmic heater, using which the gas is heated to the necessary temperature. The duration of stationary flow around the model was τ = 0.02 sec. We used a contoured nozzle with radii of the critical and outlet cross sections of 19 and 150 mm, respectively. The Mach number of the undisturbed flow in front of the model was M_∞ = 6.01 for air, and the diameter of the working part 4 was 0.5 m.

1.2. System for production of a two-phase mixture. The method of a "fluidized" bed was used for introduction of particles into the flow. For its realization, inputs with mixers were positioned at the inlet cross section of the nozzle (Fig. 2). Before the experiment, the mixer was filled with particles and then encapsulated using cover 2 and rubber seal 3. In the majority of experiments, only two of the seven inputs were used (see Fig. 1): input 1 for delivery of a dust-laden gas using the mixer and input 6 for delivery of the pure air. In the case of using just one mixer and operation in different regimes (with different types of particles, at different gas pressures in the section, etc.), the concentration of the particles in the core of the jet at the outlet from the nozzle was not absolutely constant with time. However, for the purpose of simplifying the investigation procedure, a single mixer was used in the majority of experiments.

To determine the degree of equilibrium of the motion of the gas and the particles in an undisturbed flow in front of the body, we have conducted numerical modeling of the quasi-one-dimensional flow of a dust-laden gas in the flow channel of the tunnel. The calculations have shown that SiO_2 particles of diameter d = 2 μm or smaller move in velocity and thermal equilibrium with the carrier gas in the outlet region of the nozzle (Fig. 3). With a high mass concentration of the particles (approximately more than 10%) it is necessary to take into account their influence on the parameters of the gas flow in the formed two-phase jet.

1.3. Systems of measuring the concentration. For measuring the concentration of the dust in an undisturbed flow we used the method of integral light scattering. Three different systems have been designed and used. In the first of them, a light plane (~10 mm in thickness) intersecting the jet in the transverse direction

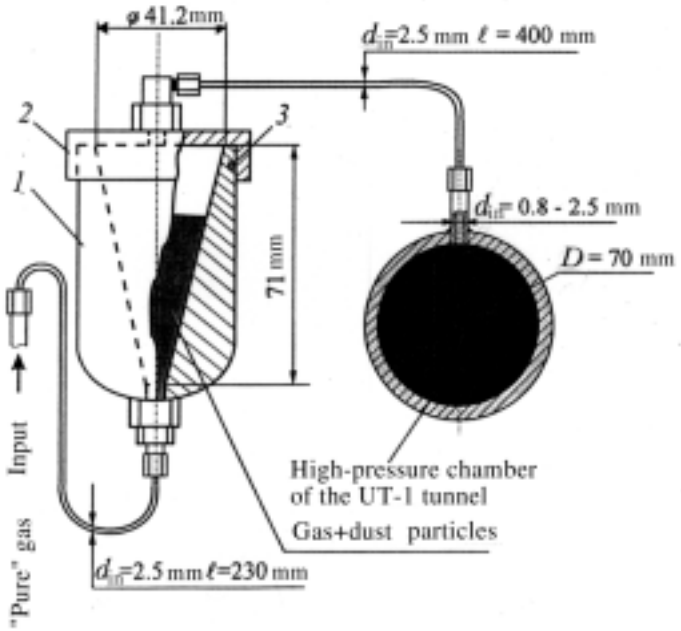

Fig. 2. Device for mixing of particles with a gas: 1) capsule; 2) cover; 3) rubber seal.

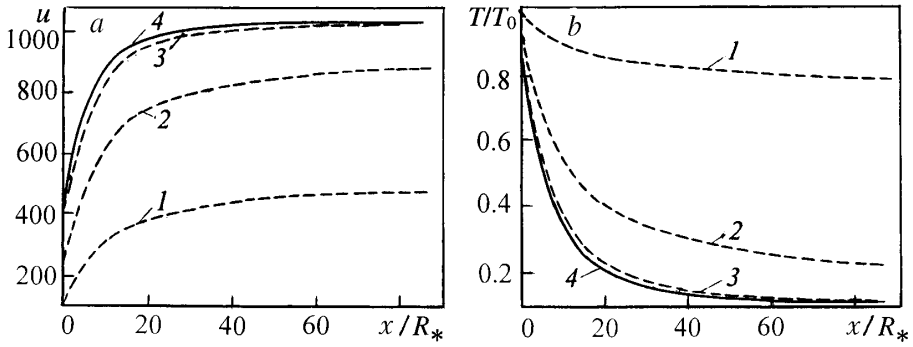

Fig. 3. Velocity (a) and thermal (b) relaxation in a nozzle (M_∞ = 6, air, T_0 = 800 K, P_0 = 10 bars, C = 0.01%): 1) d = 200, 2) 20, 3) 2 μm, and 4) gas.

is formed. For this purpose, we used an IFP-1200 high-power pulsed light source (output energy 1.2 kJ) with a duration of the flash of $\approx 10^{-6}$ sec. The background light (reflection of light from the walls of the working part of the tunnel) was depressed by a light-absorbing black screen. The light signal reflected (scattered) from the particles was recorded by a highly sensitive Panasonic SVHS NV-MS4E/NV-MS4E3 telecamera. The minimum time of exposure of a frame was $40 \cdot 10^{-6}$ sec for a frame frequency of 50 per second. The drawback of this system is strong electromagnetic interferences in operation of the pulsed light source, which introduces errors into the indications of the calorimeters for 2–4 msec.

In the alternative system, a laser of power 1 mW and wavelength 0.65 μm was used as the light source. In the majority of experiments, the light beam was directed through an optical window to a metal mirror positioned at the bottom of the working portion at the external boundary of the jet. The beam reflected from the mirror intersected the jet in the vertical direction. The intensity of the light scattered (reflected from the particles) was recorded by a black and white highly sensitive MONACOR CCD-2000 TV camera and a color SONY-SSC-370 TV camera. In the case where the laser was used, there were no errors in the indications of the calorimeters; however, when the concentration of the dust was low, the power of the light source

TABLE 1. Data on the Particles

Material	d	d_m	ρ_s	β	c_s (at T = 300 K)	Producer
SiO_2	0.15	0.19	2264	21.2	1.059	IREA
Si_3N_4	0.12	0.16	3440	16,4	≈1.000	IREA
Fe_2O_3	0.27	0.37	5250	4.10	0.881	ISFE
Cr_2O_3	0.75	1.36	5210	0.62	0.802	Baum Lux
Fe	2.40	4.6	7874	0.048	0.574	SSRICTEOC
SiO_2(h)	160	187	324	0.00082	1.059	ISA

Note. $d = [(\Sigma d_i^3 n_i)/(\Sigma n_i)]^{1/3}$, $d_m = \Sigma d_i p_i$, the parameter β was calculated for the model with a radius R = 24 mm and for the particles with a diameter d_m from the relation presented in Sec. 3 (the conditions of the tests are presented below); (h) is the hollow sphere. IREA is the Institute of Reagents; ISFE is the Institute of Solid-Fuel Enrichment; SSRICTEOC is the State Scientific-Research Institute of the Chemistry and Technology of Elementoorganic Compounds; ISA is the Baikov Institute of Steels and Alloys.

was insufficient, because of which the intensity of the recorded signal was comparable to the noise level in the equipment itself.

The third system was designed for measuring the time dependence of the concentration of the dust. A 250-W halogen incandescent lamp was used as the light source. The beam was focused to a spot ~30 mm in diameter, which was positioned in front of the model. A light detector – FD-256 photodiode – was focused on this light spot. The angle between the optical axes of the light source and the light detector was about 30°. In the process of conversion of the values of the recorded signals to the dimensions of the weight flow rate of the particles it was assumed that the dependence of the recorded signal on the weight flow rate of the particles is directly proportional; the concentration of the particles is uniform over the cross section of the jet; the mass of the powder removed by the gas flow by an instant of 0.08 sec after the breakage of the diaphragm of the tunnel is equal to the mass of the powder in the mixer before the start.

In view of the assumptions made, we can write

$$G_s = k \int_0^{0.08} J \partial\tau .$$

From this equality we determined the coefficient k for this experiment. The concentration of particles at the running instant of time was determined from the relation $C_\tau = kJ/G_g$.

1.4. Models. As models, we used four aluminum spheres with radii R = 3, 6, 12, and 24 mm, which were mounted on one holder at a distance of 41 mm from the nozzle axis. Their front surfaces were positioned in one plane perpendicular to the axis of the jet at a distance of 150 mm from the outlet cross section of the nozzle. The azimuthal angle between the spheres was 90°. A calorimetric heat-flux sensor was positioned at the critical point of each sphere.

1.5. Particles. Basic data on the particles used are presented in Table 1.

We used solid SiO_2 particles of diameter d_m = 0.19 μm and hollow particles of the same material of diameter d_m = 187 μm with a wall thickness of about 5 μm. The particles were photographed (see Fig. 4) on a PHILIPS SEM-515 scanning electron microscope at the Laboratory of Electron Microscopy of the Moscow Institute of Electronic Engineering (MIEE) by leading engineer S. V. Sedov, to whom the authors express their gratitude. The weight size distributions of the particles $S_j = \sum_{i=1}^{i=j} p_i$ were determined by measuring the images (Fig. 5). All the particles used, except for the Fe_2O_3 and Cr_2O_3 particles, had a nearly spherical shape.

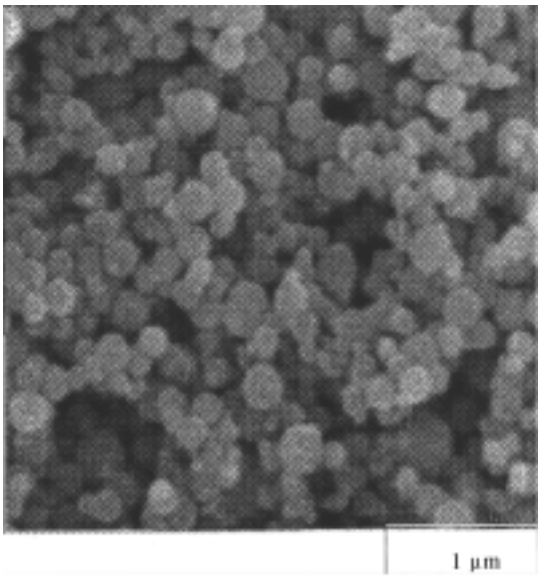

Fig. 4. Photographs of particles under the electron microscope (SiO_2, d = 0.15 μm).

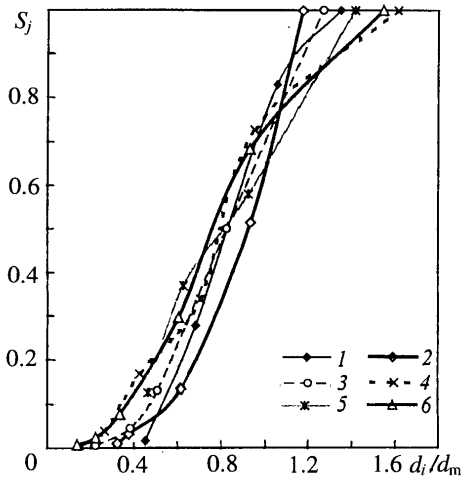

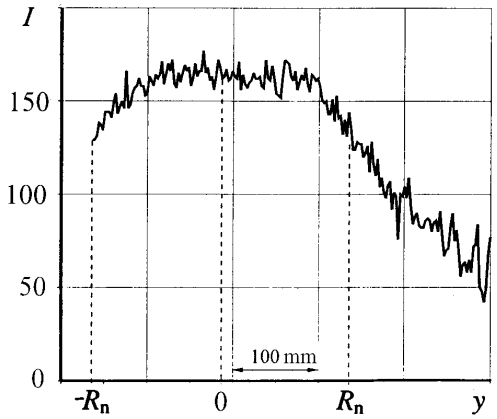

Fig. 5. Size distribution of particles: 1) SiO_2(h), 2) SiO_2, 3) Si_3N_4, 4) Cr_2O_3, 5) Fe_2O_3, and 6) Fe.

Fig. 6. Intensity of a light signal. I, V; y, mm.

Calcination of them in a heat-treating furnace has shown that all the materials used in this series of experiments are not sintered at a temperature to 600 K inclusive. We note that on long storage the particles of all the types used coagulate under the action of moisture contained in the air. In certain cases, dry particles coagulate when they are shaken in a vessel made of an electrical insulating material. To eliminate coagulation, we dried the powder of the material investigated in a thermostat at a temperature of 450 K; then we divided it into portions, wrapped them in a grounded metal foil, and stored them in an exsiccator with a $CaCl_2$ dehumidifier that provided a residual pressure of steam of no more than 0.34 mm Hg.

1.6. Conditions of the tests. The main conditions of the tests were as follows:

Working gas*	Air
Mach number (air)*	6.1
Total pressure*	17.5 bars
Stagnation temperature	570 K

TABLE 2. Varied Parameters of the Tests

Gas	Particles	d	P_0	C
Air	SiO_2	0.15	2.1	≈1
				≈25
			7.8	≈1
			17.5	≈1
				≈3
				≈6
			33.0	≈1
	Other particles		17.5	≈3
N_2, CO_2	SiO_2	0.15	17.5	≈3

Diameter of the nozzle at the outlet cross section 300 mm
Duration of the test 20 msec
Model Four spheres
Particles* SiO_2, d_m = 0.19 μm
Weight concentration of the particles in the flow* 3%

In the case of change in them, only one of the parameters denoted by the index* was varied, as a rule.

The varied conditions of the tests are presented in Table 2.

Using optical systems with a light plane and a light beam, we have recorded an approximately uniform distribution of the particle concentration in the core of the jet of diameter ≈200 mm. As an example, Fig. 6 shows results of measurement of the distribution of the intensity I of the light scattered by Fe_2O_3 particles as a function of the distance to the axis of the jet in the vertical direction with the method of a light plane. It is seen that at the boundaries of the jet the concentration of particles decreases with distance from the jet axis. The concentration of particles outside the jet is much lower than that in the core.

2. Experimental Results. Prior to the experiments with a dust-laden gas, we conducted a number of experiments in a pure air flow. It was found that for a high pressure of $P_0 \geq 7$ bars (large Reynolds number calculated from the diameter of the outlet cross section of the nozzle) and a large radius of bluntness of the model of $R \geq 12$ mm, the heat flux at the critical point of the sphere q_0 recorded in the experiments is much larger than the heat flux calculated for a laminar boundary layer at the critical point of the sphere from the Fay–Riddell formula q_c. Thus, for P_0 = 33 bars and R = 24 mm, the ratio of heat fluxes is q_0/q_c = 1.36. In all probability, such a difference in the heat fluxes is due to the presence of acoustic disturbances in the gas flow [8, 9].

In connection with the foregoing, in further analysis of the results we used the ratio of the heat flux in two-phase flow around a body to the corresponding experimentally measured heat flux in a pure gas flow q/q_0.

The rate of increase of the temperature of the calorimetric sensors was always higher in a gas flow with particles than in a pure gas. As an example, Fig. 7 shows results of measurement of the time dependence of the temperature in a gas with particles and in a pure gas. It is seen that by the end of the tests, the temperature increment (ΔT) of the dust-laden flow is about 1.5 times higher than that of the pure gas flow. It should be noted that the curve of temperature growth of the pure gas is smooth and that of the flow with particles is irregular. The latter is due to both the change in the concentration of particles during the experiment (dashed curve in Fig. 7) and electrostatic phenomena occurring near the surface of the model in the dust-laden air flow (see Sec. 4).

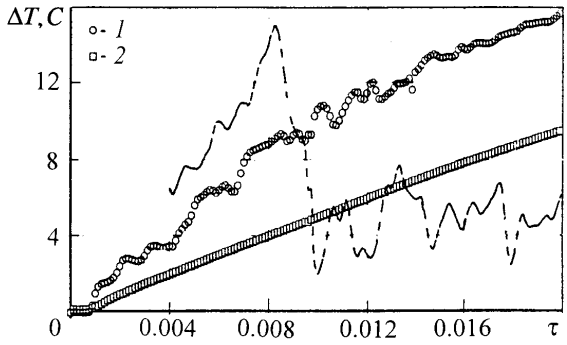

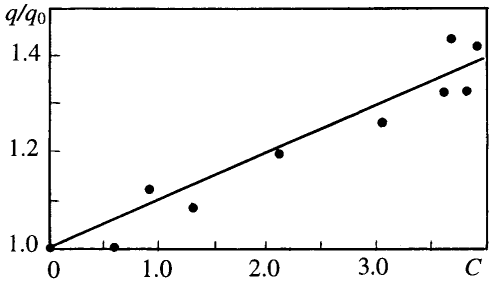

Fig. 7. Change in the calorimeter temperature [1) in a pure gas, 2) in a dust-laden gas] and in the concentration of particles (dashed curve) as a function of the time (air, SiO_2, d = 0.15 μm, R = 6 mm, P_0 = 17.5 bars).

Fig. 8. Relative heat flux at the critical point of a sphere as a function of the concentration (air, SiO_2, d = 0.15 μm, R = 6 mm, P_0 = 17.5 bars).

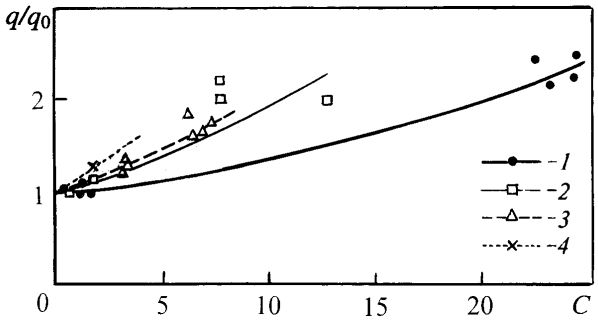

Fig. 9. Relative heat flux at different total pressures (R = 12 mm): 1) P_0 = 2.1, 2) 7.8, 3) 17.5, and 4) 33 bars.

If it is assumed that the electrical disturbances are high-frequency in character and the mean level of the additional voltage caused by them is equal to zero, for a high frequency of sampling one can significantly decrease the influence of the electrical disturbances on the heat flux recorded. This turned out to be possible in the present investigation, since the frequency of sampling of each heat-flux sensor was fairly high (8 kHz) and the resistance of the grounded wires of the measuring devices was many orders of magnitude lower than the input resistance. The dependence of the ratio of the heat fluxes on the concentration before the bow shock wave for the given experiment is shown in Fig. 8. It is seen that with a low concentration in the undisturbed gas flow the heat flux q/q_0 increases with increase in the concentration approximately linearly.

Further analysis of the results of measurements of the heat flux and the concentration of particles was made for values averaged over the time from 4 to 20 μsec. With such an averaging the influence of electrical disturbances arising in the dust-laden gas flow on the heat flux recorded decreases significantly. The results were processed without considering the initial period of time $\tau < 4$ msec, during which the nonstationary processes occurring at the stage of establishment of a regular regime can be significant. To obtain more reliable results, we repeated the experiments for each regime many times (3–6 times).

The tests have shown that the existence of even very small particles of d_m = 0.19 μm (SiO_2) in the air flow leads to a marked increase in the heat flux (Fig. 9). With a high concentration of particles ($C \geq 3\%$) in the undisturbed two-phase flow, the heat flux increases more rapidly than by a linear law. Possible reasons for the nonlinearity are discussed in Sec. 3.

The effect of enhancement of the heat flux depends nonmonotonously on the radius of the model R (Fig. 10). The largest increase in the heat flux has been revealed for a sphere with a radius R = 12 mm.

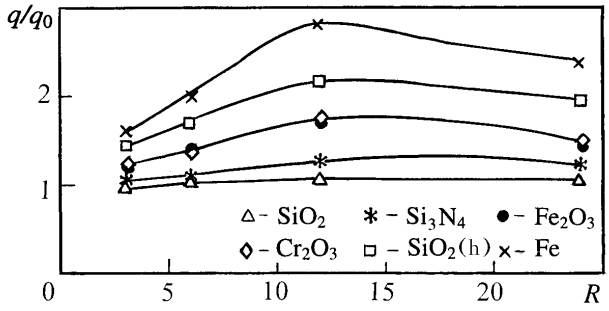

Fig. 10. Dependence of the relative heat flux on the dimensions of the model.

A larger relative heat flux q/q_0 corresponds to more inertial particles (a smaller value of the parameter β (see Sec. 3)). The exception is provided by the results for hollow SiO_2 particles (d_m = 187 μm), which is explained by a considerable lag of the velocity and the temperature of these particles behind the corresponding parameters of the gas in the jet before the bow shock wave of the model.

The influence of the composition of the gas on the heat flux was investigated only in the experiments with SiO_2 for d_m = 0.19 μm, P_0 = 17.5 bars, and C = 3%. In these tests, we used air, nitrogen (N_2), and carbon dioxide (CO_2). It has been established that the gas composition practically has no influence on the ratio of the heat flux with particles to the heat flux free of particles: compared to air, one observes only a certain tendency toward an increase in the relative heat flux in nitrogen and toward a decrease in it in carbon dioxide.

Almost in all the experiments, except for the tests with fairly inertial Fe particles (d_m = 4.6 μm), the presence of particles gave no rise to the erosion of the surface of the aluminum models.

3. Comparison to Numerical Investigations. Analysis of the experimental conditions shows that most of the results obtained with SiO_2 particles of d_m = 0.19 μm for models with a large radius R are appropriate for the so-called "regime without inertial precipitation of particles": in this regime, low-inertia particles are retarded practically completely in the shock layer and do not find their way to the surface of a body. For such a regime of flow, the heat flux to the critical point of the body can be calculated without empirical information (necessary in the case of the contact heat exchange particle–wall) within the framework of the theory of a laminar two-phase boundary layer which is based on the two-liquid model of a dust-laden gas [6, 10]. The boundaries of the regime without inertial precipitation of particles in hypersonic two-phase flow around a sphere for the conditions of continuous flow around particles have been determined in [6].

In the present investigation, the boundaries of the regime of inertial precipitation have been determined numerically by a method analogous to [6], but with consideration of the Knudsen effects in the case of flow around particles. Figure 11 shows a calculated curve separating the regime of flow with a precipitation of particles from the regime without precipitation in the coordinates of the dimensionless parameters:

$$\beta = (27\mu_c R)/(d^2 u_\infty \rho_s \phi), \quad \mathrm{Rb} = (1/6)\,(d\rho_c u_\infty/\mu_c)^{2/3}.$$

Here β is the parameter equal to the ratio of the dimension of the body in flow to the length of the velocity relaxation of a particle in the case of the Stokes law of resistance of a sphere as corrected for the finiteness of the Knudsen effects, Rb characterizes the deviation of the law of resistance of a particle from the Stokes law, and ϕ is the correction factor accounting for the influence of the finiteness of the Knudsen number (Kn) on the resistance of a particle [11]:

$$\phi = 1 + \mathrm{Kn}\,(2.492 + 0.84 \exp(-1.84/\mathrm{Kn})), \quad \mathrm{Kn} = l_\lambda/d, \quad l_\lambda = (1.255\mu_c)/(\rho_c T_c^{0.5} \mathrm{Rb}^{0.5}),$$

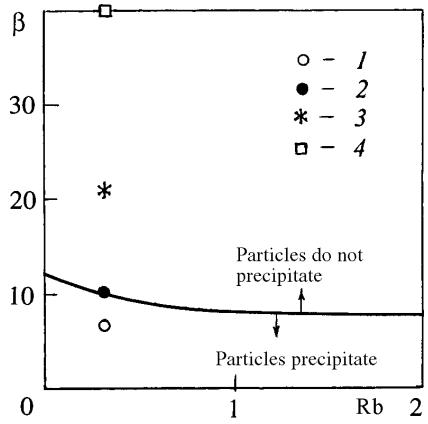

Fig. 11. Boundaries of the regime of inertial precipitation: 1) R = 3, 2) 6, 3) 12, and 4) 24 mm.

where l_λ is the mean free path of gas molecules near the stagnation point of a nonviscous flow (at the external boundary of the boundary layer).

The points in Fig. 11 correspond to the values of the dimensionless parameters calculated for the conditions of experiments with spherical models in flow of air with SiO_2 particles of maximum diameter d = 0.22 μm (the calculations have shown that large particles make the main contribution to the increase in the heat flux). The increase in the value of the ordinate of a point corresponds to the increase in the radius of the model R = 3, 6, 12, and 24 mm. According to the calculation, particles must precipitate on the sphere of R = 3 mm. The conditions for the sphere with R = 6 mm actually coincide with the boundary of the regime with precipitation of particles, and the regime without inertial precipitation of particles is realized for the spheres of R = 12 and 24 mm.

In the calculations of the gas parameters in the shock layer, we used the asymptotic hypersonic solution "with a constant density" [12], and the resistance of a particle was calculated with the use of expressions from [16], but with the indicated corrections to the coefficient of resistance of particles for the finiteness of the Knudsen number. As has been shown by numerical methods in [6, 13], in the case of flow around a blunt body in the regime without precipitation, particles are accumulated near the front surface of the body. As a result, the local mass concentration of particles in the boundary layer becomes significant, which, in combination with the excess of the temperature of the particles over the temperature of the gas, leads to the "filling" of the profile of the gas temperature in the boundary layer and to an increase in the heat fluxes at the critical point of the body.

Details of the mathematical model of a nonviscous shock layer and of the equations of a two-phase boundary layer on a blunt body as well as the description of the numerical procedures are presented in [6, 13]. Here, we give only some of the results of the numerical investigation of the heat flux at the stagnation point in comparison with the experimental data for SiO_2 particles; we performed calculations on the assumption that the particles are monodisperse and have a diameter d_m. The other parameters of the gas and of the particles were taken the same as in the experiment (see Sec. 1).

Figure 12a shows results of calculation of the relative heat flux to the critical point of the sphere of R = 6 mm as a function of the mass concentration of particles in an undisturbed flow. Curve 1 corresponds to the calculations within the framework of the theory of a two-phase boundary layer for the regime without inertial precipitation of particles [6]; the points denote experimental data. Curve 2 shows the maximum possible increase in the heat flux, which can be realized in the limit of very inertial particles ($\beta \to 0$) which are not retarded in the shock layer and on the assumption that the entire energy of the particles is used for heating the surface in flow:

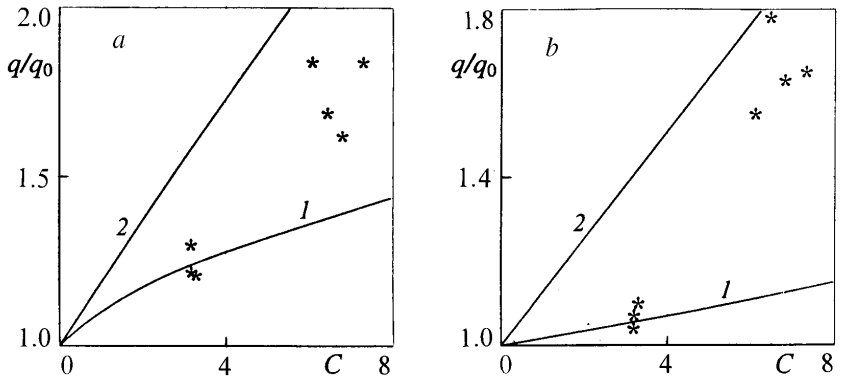

Fig. 12. Comparison of the calculated and experimental data for the heat exchange at the critical point of a sphere [R = 6 mm (a), 3 mm (b]: 1) calculation and 2) limiting heat flux; the points denote experiment.

$$q_{\max} = c_{\infty}\rho_{\infty}u_{s\infty}\,(u_{s\infty}^2/2 + (c_{s\infty}T_{\infty} - c_{sw}T_w). \qquad (1)$$

Figure 12b compares the calculated and experimental data for the relative heat fluxes at the critical point of the sphere of R = 3 mm. According to Fig. 11, for this radius of a sphere, the regime with precipitation of particles must be realized; therefore, in this case, the heat flux from the particles was calculated from formula (1), but in place of the particle parameters in an undisturbed flow (with the index ∞), we used the values of the parameters calculated at the critical point of the sphere with account for the retardation of particles in the shock layer (curve 1). Curve 2, as in the preceding figure, shows the maximum possible increase in the heat flux. The heat fluxes from the carrier phase were calculated using the equations of a boundary layer in a pure gas. It should be noted that, as applied to the experimental conditions, the heat capacity of SiO_2 particles changes significantly when the temperature varies: from c_s = 0.2 kJ/(kg·K) at 80 K to c_s = 1.0 kJ/(kg·K) at 600 K.

As is seen from Fig. 12, the calculated and experimental results agree satisfactorily for low mass concentrations of the particles in an undisturbed flow, approximately to C = 3%. For high concentrations of the particles before the wave (the particle concentration near the surface of a body is many times higher) the experimental points lie higher than the calculated curves, which can be due to several reasons, including the influence of the particles on the parameters of the nonviscous flow as well as the existence of collisions between particles having different sizes and the possibility of coagulation of particles. These reasons can cause an increase in the effective size (inertia) of particles and, as a consequence, an increase in the additional heating of the body.

It should be noted that there are also other experimental factors which make the direct comparison of theoretical and experimental results difficult, among them the polydispersity, the nonspherical shape of particles, the existence of electric charge on the particles, and others. Because of this, the present investigation should be considered as only the beginning of a detailed investigation of the intensification of the heat exchange in high-speed flows containing microparticles. However, the experimental and theoretical results presented testify that the existence of even low-inertia particles (which do not precipitate on the surface of a body) can cause a significant increase in the heat flux in the region of retardation on a blunt body moving in a dust-laden atmosphere.

4. Optical Phenomena. Some experiments were conducted in total darkness (in the absence of a light source in the building and in the working portion of the tunnel). In this case, there was a marked glow near the front surface of the models (Fig. 13). Additional experiments have shown that a laser beam introduced into the working portion has practically no influence on the intensity of the glow of the flow near the surface.

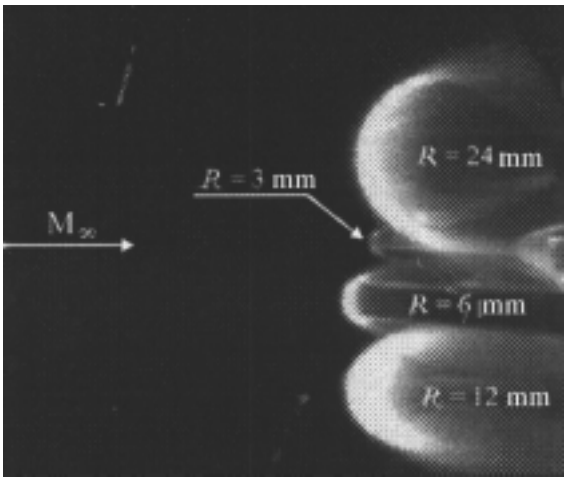

Fig. 13. Optical radiation in the case where models were in the flow of a dust-laden gas (air, P_0 = 17 bars, Fe, d = 2.4 mm, C = 3%).

It was established using a color TV camera that in the overwhelming majority of experiments the flow radiated white light with a bluish tint.

The intensity of the glow decreased with decrease in the density and size of the particles as well as their concentration. Optical effects were observed with air (in the overwhelming majority of experiments) and also with N_2 and CO_2. The glow was completely absent in a pure (without particles) flow.

A significantly weaker glow was also observed near the walls of the nozzle, especially in the region of separation of the flow from its edge, and near the surface of the devices in the working portion of the tunnel.

In the case where the measuring routes of the calorimeters were not grounded, electrostatic voltage (≈20 V or more) appeared in the measuring circuits at the input of the amplifier, which put the amplifier of the calorimetric circuits out of action. Because of this, in further experiments the calorimeters and the body of the model were grounded, but this caused significant electric interferences in the measuring circuits of the calorimeters.

Electric charges on the particles are most probably due to the friction of particles against each other and against the walls of the channel in the process of preparation of a two-phase mixture in a high-pressure chamber and also, apparently, due to the friction of particles against the surface of the model.

Such effects should be expected in the case where spacecraft move in an atmosphere containing condensed particles, in particular, when spacecraft enter the atmosphere of the Mars [14]. Electric discharges can make electronic equipment on a spacecraft inoperative, which generates the need for further investigation of electrical and electrooptical phenomena in high-speed gas-dust flows around bodies. Such phenomena can also be of significance in spraying of a condensed phase on the surface of products and in other processes.

Conclusions. Experimental investigations conducted in a shock wind tunnel have shown that the presence of small particles (with a size of the order of a micron or fractions of a micron) in a hypersonic flow causes a significant increase in the heat flux (to three times) to the front surface of a body in flow even with a low mass concentration of the particles (of the order of several percent).

With low mass concentrations of dust, the effect of enhancement of heat exchange is weakly related to the composition of the carrier phase (C_2, N_2, air) and depends nonmonotonously on the radius of the model. The heating of a model increases with increase in the inertia of the particles and their mass concentration.

Based on the numerical calculations of flow of a nonviscous hypersonic dust-laden gas around a sphere, we have determined the boundaries of the region of dimensionless determining parameters corre-

sponding to the absence of precipitation of particles on the surface of the sphere. It is shown that the majority of experimental results for SiO_2 particles (d_m = 0.19 μm) correspond to the regime without precipitation of particles, which is also evidenced by the absence of erosion on the surface of the models. The numerical calculations of the heat flux at the stagnation point on the sphere for small values of the mass concentration of the particles are in agreement with the experimental data.

It has been revealed that in the absence of external light sources there is a glow near the front surface of the model. An electric potential arises in the measuring circuits of the calorimeters of the model, which are not connected to ground. The grounding of the calorimeter causes a significant noise in its measuring circuits. These effects were not observed in the experiments without particles.

This work was carried out with partial financial support from the International Science and Technology Center (project 1549), the Russian Foundation for Basic Research (RFBR), and the Russian Foundation for Basic Research and the National Science Foundation of China (NSF of China) (joint project 99-01-39020NSF-a).

NOTATION

μ, viscosity, kg/(m·sec); ρ, density, kg/m^3; τ, time, sec; β, parameter of velocity relaxation; Φ, correction factor of the resistance of a particle; ρ_s, density of the material of particles, kg/m^3; C, weight concentration, %; c_s, heat capacity of the material of particles, kJ/(kg·K); d, diameter of particles, μm; d_m, weighted-mean diameter of particles, μm; G_g, flow rate of the gas through the critical cross section of the nozzle, kg/sec; G_s, weight of particles in the mixer before the experiment, kg; J, running value of the signal recorded after the amplifier, V; k, coefficient constant for given conditions of the experiment, kg/(sec·V); l_λ, mean free path of a gas molecule, μm; M, Mach number; n_i, number of particles of a given diameter; P, pressure, bars; p_i, weight fraction of particles of a given size of the total mass of particles; q, heat flux, W/cm^2; q_0, heat flux at the critical point in the absence of particles, W/cm^2; R, radius, mm; R_*, radius of the nozzle in the critical cross section, mm; Rb, parameter of aerodynamic resistance of particles; $\mathrm{Re}_{\infty,R}$, Reynolds number calculated from the parameters of the undisturbed flow and the radius of the model; R_g, gas constant, kJ/(kg·K); R_n, radius of the nozzle in the outlet cross section, mm; S_j, weight-distribution parameter; T, temperature, K; T_w, temperature of the wall, K; I, intensity of the light signal; u, velocity, m/sec; x, distance along the axis of the nozzle from its critical cross section, mm; y, direction along the vertical from the axis of the nozzle, mm; d_{in}, inside diameter, mm; l, length, mm. Subscripts: c, forward critical point; s, particles; ∞, undisturbed flow; 0, isentropic deceleration; g, gas, m, weighted-mean; w, wall; in, inside.

REFERENCES

1. J. A. C. Humphey, *Int. J. Heat Fluid Flow*, **11**, No. 3, 170–195 (1990).
2. D. S. Mikhatulin, Yu. V. Polezhaev, and I. V. Repin, *Heterogeneous Flows: Gasdynamics, Heat Transfer, and Erosion*, Preprint No. 2-402 of the Institute of High Temperatures of the Russian Academy of Sciences [in Russian], Moscow (1997).
3. W. A. Fleener and R. H. Watson, *Convective Heating in Dust-Laden Hypersonic Flows*, AIAA Pap. No. 73-761 (1973).
4. L. E. Dunbar, J. F. Courtney, and L. D. McMillen, *AIAA J.*, **13**, No. 7, 908–912 (1975).
5. W. C. L. Shin, *Ballistic Range Measurements of Aerodynamic Heating in Erosion Environments*, AIAA Pap. No. 76-319 (1976).
6. A. N. Osiptsov and E. G. Shapiro, *Izv. Akad. Nauk SSSR, Mekh. Zhidk. Gaza*, No. 5, 55–62 (1986).
7. V. Ya. Bezmenov and Yu. Yu. Kolochinskii, *Structure and Characteristics of a UT-1 Hypersonic Shock Tunnel Designed at the Central Aerohydrodynamics Institute, Tr. TsAGI*, No. 9152 (1969).

8. V. Ya. Borovoy, A. Yu. Chinilov, V. N. Gusev, I. V. Struminskaya, L. Delery, and B. Chanetz, *AIAA J.*, **35**, No. 11, 1721–1728 (1977).
9. A. R. Wieting and M. S. Holden, *AIAA. J.*, **27**, No. 11, 1557–1565 (1989).
10. A. N. Osiptsov, *Appl. Mech. Rev.*, **50**, No. 6, 357–370 (1997).
11. N. A. Fuchs, *The Mechanics of Aerosols*, New York (1964).
12. W. D. Hayes and R. F. Probstein, *Hypersonic Flow Theory*, Academic Press, New York (1959).
13. A. N. Osiptsov and E. B. Vasilevskii, in: *Proc. 2nd Int. Symp. Two-Phase Flow Model. Experim.*, May 23–26, 1999, Pisa, Vol. 3, Italy (1999), pp. 1893–1900.
14. J. C. Kolecki, B. Hillard, and M. Sielbert, *Overview of Mars System–Environment Interactions*, AIAA Pap. No. 96-2333 (1996).